US-APWR Incore Power Distribution Evaluation Methodology

Non-Proprietary Version

December 2007

(This page is intentionally left blank.)

Revision History

Revision	Page	Description
0	All	Original issued

Mitsubishi Heavy Industries, Ltd.
16-5, Konan 2-chome, Minato-ku
Tokyo 108-8215 Japan

Abstract

This report describes the method for determination of the incore power distribution to be used in the US-APWR core. Using the same method employed for Japanese Mitsubishi PWRs, incore power distribution measurements are periodically performed for core operation management and for surveillance as described in the Technical Specifications.

A summary description of the INCORE-M code method, which is used for measurement data processing, is given. In addition, uncertainty factors evaluation results are provided in this report. Many of the uncertainties applied to the US-APWR using INCORE-M are identical to values applied to other PWRs using this method. However, the unique US-APWR design feature has been considered when determining total uncertainty factors.

It is concluded that the appropriate uncertainty on power peaking factors are applied to the US-APWR safety analyses and core surveillance.

Table of Contents

List of Tables

List of Figures

List of Acronyms

APWR	Advanced Pressurized Water Reactor
BOC	Beginning of Cycle
BA	Burnable Absorber
EOC	End of Cycle
HFP	Hot Full Power
HSI	Human-System Interface
I&C	Instrumentation and Control
ICIS	Incore Nuclear Instrumentation System
MD	Movable Fission Chamber Detector
MHI	Mitsubishi Heavy Industries, LTD.
MOC	Middle of Cycle
NRC	Nuclear Regulatory Commission
PWR	Pressurized Water Reactor
RPI	Rod Position Indication

1.0 INTRODUCTION

This report describes the power distribution evaluation methodology for the US-APWR. Using the same methods employed for Japanese Mitsubishi PWRs, which are based on Westinghouse-type PWR technology, incore power distribution measurements are periodically performed for the purpose of core operation management and to satisfy surveillance requirements as described in the Technical Specifications.

The incore power distribution is determined by taking a flux map of the core, obtained by the incore nuclear instrumentation system (ICIS) described in this report. The incore power distribution evaluation methodology applied for US-APWR has extensive experience in Japan, and has been applied for all Mitsubishi PWRs (23 units, representing more than 300 first and reload cycles).

In this report, Chapter 2 briefly introduces the ICIS of the US-APWR. Chapter 3 describes the methodology to determine the measured power distribution, and Chapter 4 describes INCORE-M, the computer code for power distribution determination. Finally, Chapter 5 discusses the measurement uncertainties on power peaking factors.

Additionally, Appendix-A discusses the effect of reducing the available instrument thimbles for the US-APWR.

2.0 SUMMARY OF INCORE NUCLEAR INSTRUMENTATION SYSTEM

Movable fission chamber detectors (MDs) can be remotely positioned in the core through guide thimbles to provide flux mapping of the core. The detector guide thimbles penetrate the reactor vessel closure head through seal assemblies and terminate at the bottom of the fuel assemblies. The detector guide thimbles extend from the bottom of the fuel assemblies to the detector drive unit in the containment vessel. The detector guide thimbles are distributed over the core nearly uniformly. Configuration of the main components of the system for insertion and withdrawal of these detectors is shown in Figure 2-1.

The thimble assemblies, which integrate the several detector guide thimbles, are mounted on the upper core support plate as shown in Figure 2-1.

The main components of the system for insertion and withdrawal of the detectors are drive units and path selector assemblies, as shown in Figure 2-1. The drive system pushes hollow helical wrap drive cables into the core with the detectors attached to the leading ends of the cables and small diameter coaxial cables threaded through the hollow centers back to the end of the drive cables. Each drive unit consists of motors and storage wheels that accommodate the total drive cable length. The motor pushes a helical drive cable and a detector through a selected thimble path by means of the path selectors. Every thimble location can be accessed by each detector controlled from different drive units. A common path is provided for cross-calibration of the detectors.

The incore nuclear instrumentation data acquisition and drive motor control equipment are located inside the non-safety instrumentation and control (I&C) equipment room.

The incore nuclear instrumentation Human-System Interface (HSI) is located inside the I&C equipment room. This HSI provides means for manually or automatically inserting and withdrawing the detectors and recording neutron flux data from the detectors. The control and readout system consists of the necessary equipment for control, position indication, and flux recording for each detector.

A flux mapping consists of selecting thimbles in given fuel assemblies at various core locations. Signals from the detectors are recorded as the detectors are repositioned in the core. A plot of position versus neutron flux levels is provided from this data. In a similar manner, other core locations are selected and scanned. Flux mappings are conducted periodically in accordance with Technical Specification surveillance requirements. The recorded data are used as input for the core power distribution evaluation code, INCORE-M, which is described in Chapter 4 of this report.

Figure 2-2 shows the radial distribution of instrument thimbles for the US-APWR. A total of 37 instrument thimbles are distributed nearly uniformly in the core. The distribution of instrument thimbles in each quadrant is nearly identical.

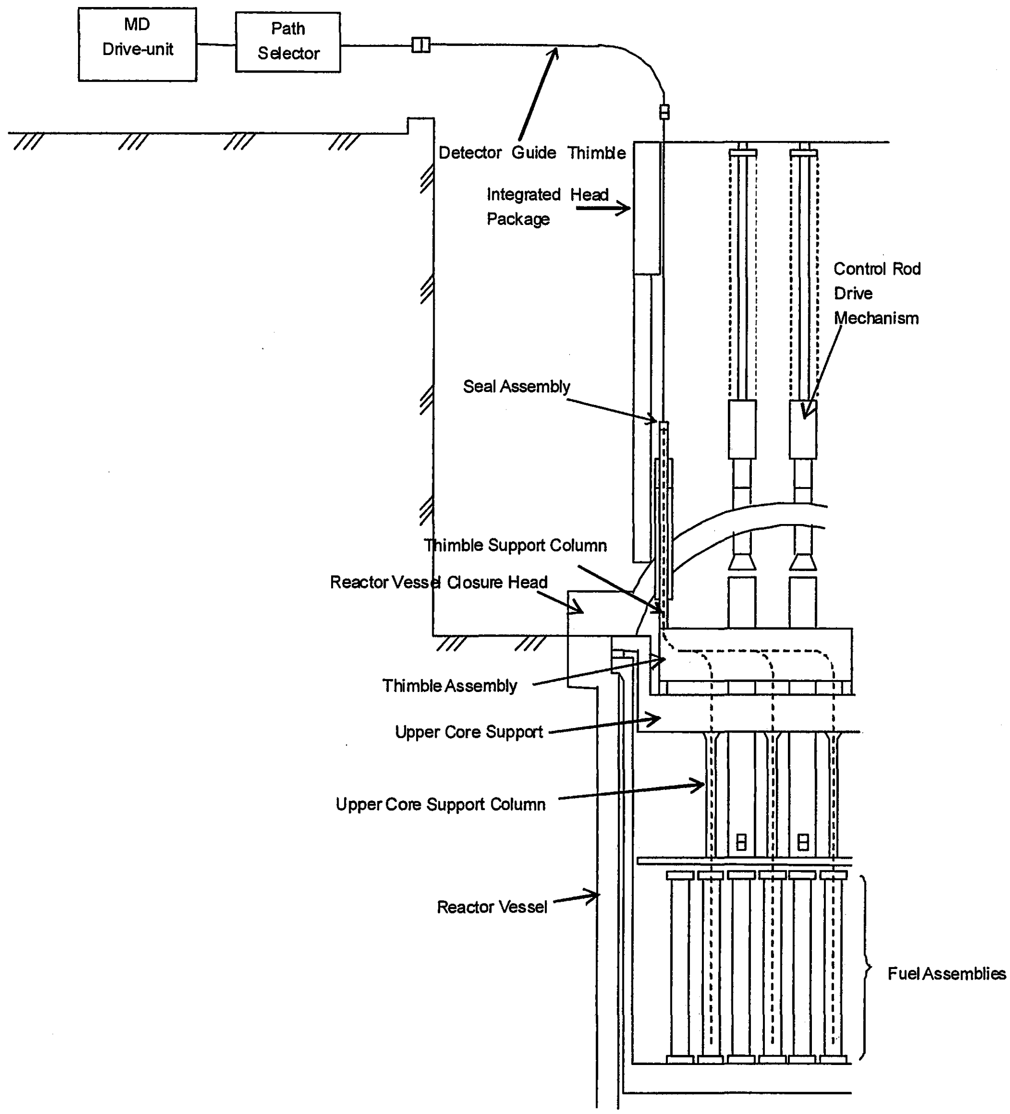

Figure 2-1 Basic System for Insertion of Movable Neutron Detectors

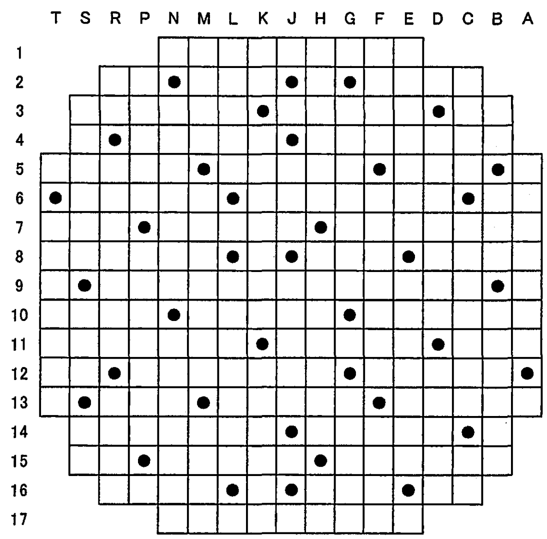

● : Instrument thimbles (37)

Figure 2-2 Radial Distribution of Instrumented Locations for the US-APWR

3.0 INCORE POWER DISTRIBUTION DETERMINATION METHOD

This chapter shows the method used for the incore power distribution determination in the US-APWR. This method is same as the one used in the conventional PWRs. The outline of the ICIS in US-APWR is shown in Chapter 2. The principle of the flux mapping is same and [ ]. The same methodology used in the conventional PWRs, therefore, can be applied to the US-APWR.

3.1 MD Data Processing

The incore power distribution is evaluated using flux traces measured by MDs axially through the instrumentation thimbles of selected fuel assemblies. [ ]

These point-wise [ ] readings are converted to point-wise MD reaction rates and are corrected [ ] by the following relationship.

[ ]

Normally, several detectors are used for the flux mapping. To correct the difference of sensitivity between detectors, each detector is routed separately in a common calibration thimble at least once. [ ]

[ ]

[ ]

3.2 Source Deck

Together with the measured MD signal data described in Section 3.1, predicted data are also used to evaluate the incore power distribution. The predicted data input is called "source deck" and includes predicted values of [ ] Section 4.2 includes a detailed listing of information included in the source deck. Source decks are based on the three dimensional (3D) core calculations that simulate the core conditions during incore flux trace measurement. [ ]

The incore power distribution varies with core depletion; therefore, [ ] Furthermore, control rod insertions affect the incore power distribution, and therefore [ ] For power distribution evaluations, suitable source decks are selected based on the appropriate conditions when the incore flux distribution measurement is performed.

3.3 Incore Power Distribution Determination

For each axial mesh point "k", assembly average powers and fuel rod powers are determined by the following relationship using measured MD reaction rates and source decks. Assembly average and fuel rod powers in uninstrumented assembly are extrapolated using measured data in the vicinity of the assembly.

$$MP_{k,i} = \sum_{j} W_{i,j} \cdot \frac{PP_{k,i}}{PR_{k,j}} \cdot MR_{k,j}\ , \qquad (3\text{-}3)$$

where $MP_{k,i}$: Evaluated assembly-average power or fuel rod power in assembly i at axial location k,

$PP_{k,i}$: Predicted assembly-average power or fuel rod power in assembly i at axial location k ,

$PR_{k,j}$: Predicted MD reaction rate in assembly i at axial location k, calculated by the product of MD reaction cross section (U-235 fission reaction cross section in detector) σ_j and flux in instrumentation thimble $\phi_{k,j}$ at axial location k in instrumented assembly j,

$MR_{k,j}$: Measured MD reaction rate in instrumented assembly j at axial location k, described in Section 3.1,

$W_{i,j}$: Weighting function determined according to the distance[

]

$W_{i,j}$[ ]and are normalized as $\sum_{j} W_{i,j} = 1$.

The incore power distribution determined by Equation 3-3 is normalized for reactor average power to be unity. This relative distribution is collapsed axially and compared with the predicted distribution to confirm the validity of design calculations and the relative fuel rod power distribution is used to determine power peaking factors described in the next section.

3.4 Power Peaking Factor Evaluation

Power peaking factors are evaluated based on the relative fuel rod power distribution as described below.

The nuclear enthalpy rise hot channel factor for fuel rod n; $\left(F_{\Delta H}^{N}\right)_n$ is defined as the ratio of the integrated fuel rod power to the average fuel rod power in the core. The average fuel rod power and $\left(F_{\Delta H}^{N}\right)_n$ are evaluated by the following equations.

$$\overline{P} = \sum_i \left(f_i \cdot \sum_k MP_{k,i} \right) \Big/ \sum_i f_i , \tag{3-4}$$

where $\overline{P}$: Average fuel rod power in the core,

$MP_{k,i}$: Evaluated assembly power of assembly i at axial location k,

f_i : Number of fuel rods in assembly i,

$$\left(F_{\Delta H}^{N}\right)_n = \sum_k MP_{k,n} \Big/ \overline{P} , \tag{3-5}$$

where $MP_{k,n}$: Evaluated power of fuel rod n at axial location k.

The axial peaking factor for fuel rod n; $\left(F_Z\right)_n$ is defined as the maximum value in axial power profile of the fuel rod and power evaluated by

$$\left(F_Z\right)_n = \frac{\underset{k}{\mathrm{Max}}\left(MP_{k,n}\right)}{\overline{MP}_n} , \tag{3-6}$$

where $\overline{MP}_n$: Average of $MP_{k,n}$ over the core height.

Furthermore, the nuclear heat flux hot channel factor for fuel rod n; $\left(F_Q^N\right)_n$ is defined as the maximum local heat flux divided by the average fuel rod heat flux assuming nominal fuel pellet and rod parameters. $\left(F_Q^N\right)_n$ is evaluated by a product of $\left(F_{\Delta H}^{N}\right)_n$ and $\left(F_Z\right)_n$;

$$\left(F_Q^N\right)_n = \left(F_{\Delta H}^{N}\right)_n \cdot \left(F_Z\right)_n , \tag{3-7}$$

and the heat flux hot channel factor for fuel rod n; $\left(F_Q\right)_n$ is evaluated by multiplying $\left(F_Q^N\right)_n$ by the engineering heat flux hot channel factor F_Q^E;

$$\left(F_Q\right)_n = \left(F_Q^N\right)_n \cdot F_Q^E . \tag{3-8}$$

4.0 INCORE-M CODE

4.1 General Description

The INCORE-M code, which integrates the methodology described in Chapter 3 is used to determine the incore power distribution in the US-APWR. INCORE-M is modified based on the INCORE code (Reference 1) for the US-APWR application, for example the applicable core geometry is enhanced to the core of 257 fuel assemblies. INCORE-M generates solutions equivalent to that of INCORE.

4.2 Input Data

INCORE-M uses the following input data.

(1) Options

- Plant description (2, 3, 4-loop Westinghouse- type cores and US-APWR)
- Specification for calculational model, desired output, etc.

(2) Core conditions when a flux mapping is performed

(3) MD data

- MD reaction rate data measured with ICIS (described in Section 3.1)

(4) Source decks

4.3 Output Data

INCORE-M edits the following information.

(1) Echoes of input data

(2) MD data

(3) Evaluated incore power distribution

Figure 4-1 Example of INCORE-M Output
(MD Data used for Power Distribution Determination)

Figure 4-2 Example of INCORE-M Output (Axial Power Distribution)

Figure 4-3 Example of INCORE-M Output (Radial Power Distribution)

Figure 4-4 Example of INCORE-M Output (Top Twenty of F_Q)

Figure 4-5 Example of INCORE-M Output (Axial Profile of F_Q)

Figure 4-6 Example of INCORE-M Output (Summary)

5.0 UNCERTAINTY EVALUATION FOR POWER PEAKING FACTORS

5.1 General Description of Uncertainty Analysis

Derivations of uncertainties for power peaking factors ($F_{\Delta H}^{N}$ and F_{Q}^{N}) for Westinghouse-type PWRs are described in depth in Reference 2, which was approved by NRC. For the US-APWR, methodologies to infer the incore power distribution is basically the same as Westinghouse-type PWR as described in Chapters 3 and 4.

The only major difference between US-APWR and Westinghouse-type PWR regarding input conditions for the uncertainty analysis is the radial deployment of the instrumentation thimbles in the core.

For Westinghouse-type PWRs, approximately 30% of the fuel assemblies in the core are typically instrumented. In contrast, 37 out of the total 257 fuel assemblies (14.4%) are instrumented for US-APWR as shown in Figure 2-2 of Chapter 2. Therefore, the measurement uncertainties are re-evaluated considering the configuration of the US-APWR measured instrumentation thimble locations. The difference in available measured instrumentation thimbles affects uncertainties for measurement extrapolation and the allowance for thimble failures.

In this chapter, the methodology to evaluate the uncertainties of power peaking factors and the results are discussed.

5.2 Methodology of Uncertainty Analysis

In Reference 2, the process to obtain power peaking factor is analyzed and several uncertainty components are defined, which are evaluated individually. The total uncertainties on $F_{\Delta H}^{N}$ and F_{Q}^{N} are determined by combining these uncertainty components. A brief summary of the evaluation methodology in Reference 2 is provided below.

The measured hot rod power ($F_{\Delta H}^{N}$) can be expressed as Equation 5-1:

$$\mathrm{MP}(x,y)=C\cdot\sum_{x',y'}\left\{\overset{(1)}{\mathrm{MR}(x',y')}\cdot\overset{(2)}{\frac{\mathrm{PP}^{assembly}(x,y)}{\mathrm{PR}(x,y)}}\times\overbrace{W(x,y,x',y')\cdot\frac{\mathrm{PR}(x,y)}{\mathrm{PR}(x',y')}}^{(3)}\cdot\overset{(4)}{\frac{\mathrm{PP}^{rod}(x,y)}{\mathrm{PP}^{assembly}(x,y)}}\right\}, \qquad (5\text{-}1)$$

where, MP(x,y):	Measured power of the hot rod in fuel assembly (x,y),
MR(x',y'):	Measured reaction rate integral over height in instrumented fuel assembly (x',y'),
$PP^{rod}(x,y)$:	Predicted power of the hot rod in fuel assembly (x,y),
$PP^{assembly}(x,y)$:	Predicted average power of fuel assembly (x,y),
PR:	Predicted reaction rate,
W(x,y,x',y'):	The Weighting function defined in Chapter 3,
C:	A constant for normalization.

Also, the measured local power peaking ($F_Q^N(z)$) can be expressed as Equation 5-2:

$$\begin{aligned}\mathrm{MP}(z) &= C\cdot\underset{\text{over}\,x,y}{\mathrm{Max}}\{\mathrm{MP}(x,y,z)\}\\ &= C\cdot\underset{\text{over}\,x,y}{\mathrm{MAX}}\left\{\sum_{x',y'}\left(\overbrace{\mathrm{MR}(x',y')\cdot W(x,y,x',y')\cdot\frac{\mathrm{PP}^{rod}(x,y)}{\mathrm{PR}(x',y')}}^{(\mathrm{I})}\times\overbrace{\underset{(5)}{\frac{\mathrm{PP}^{rod}(x,y,z)/\mathrm{PR}(x',y',z)}{\mathrm{PP}^{rod}(x,y)/\mathrm{PR}(x',y')}}\cdot\underset{(6)}{\frac{\mathrm{MR}(x',y',z)}{\mathrm{MR}(x',y')}}}^{(\mathrm{II})}\right)\right\},\end{aligned} \qquad (5\text{-}2)$$

where all the variables retain the previous definitions except that some of the variables are height (z) dependent here. Term (I) of Equation 5-2 is identical to Equation 5-1, which defines $F_{\Delta H}^N$.

The following six uncertainty components consistent with Equations 5-1 and 5-2 are then defined:

(1) Radial Measurement Reproducibility Uncertainty
(2) Predicted Power to Reaction Rate Uncertainty
(3) Extrapolation Uncertainty from Instrumented to Uninstrumented Fuel Assembly
(4) Predicted Radial Local Peaking Uncertainty
(5) Predicted Elevation Dependent Power to Reaction Rate Uncertainty
(6) Axial Measurement Reproducibility Uncertainty

Therefore, the measurement uncertainty on $F_{\Delta H}^{N}$ can be evaluated as a combination of the uncertainty components (1) to (4), and a combination of the components (1) to (6) results in the measurement uncertainty on F_{Q}^{N}.

As stated in Section 5.1, the main difference regarding incore power distribution measurement conditions between US-APWR and Westinghouse-type PWRs is the distribution and the fractions of measured instrumentation thimbles. Therefore, for all components except component (3), the same values evaluated in Reference 2 are applicable to US-APWR for the following reasons:

- Components (1) and (6) are accuracies of the detectors, and are not dependent on the deployment of instrument thimbles in the core.

- Components (2) and (4) are errors associated with the nuclear calculational codes, and are not dependent on the deployment of instrument thimbles. PARAGON/ANC (References 3, 4 and 5) are used for the US-APWR nuclear design calculations. PARAGON/ANC has been previously approved with the use of the uncertainties in Reference 2.

- Component (5) is not dependent on the deployment of instrument thimbles; it is related to the nuclear design method used to supply source deck for INCORE-M (see Section 4.2). For the US-APWR, the source deck is supplied by ANC, and multiple axial regions are considered as described in Chapter 3. Therefore, the uncertainty on component (5) is bounded by the value in Reference 2, which was evaluated based on using single axial region source deck.

As a result, only component (3) of Equation 5-2 (the extrapolation uncertainty) must be re-evaluated under the specific conditions of the US-APWR. In the next section, the method used to evaluate the extrapolation uncertainty is described.

5.3 Extrapolation Uncertainty Evaluation

5.3.1 Method

As described in Reference 2, the extrapolation uncertainty, E^{ext}, is defined in Equation 5-3:

$$E^{ext} = \left(\frac{P^{ref}}{P^{ext}} - 1\right) \times 100 \quad , \qquad (5\text{-}3)$$

where, P^{ref} is an assembly power (or hot rod power) determined without the extrapolation method described in Chapter 3, and P^{ext} is that determined with extrapolation. These powers can be evaluated by performing INCORE-M power distribution calculations twice for the same set of data and comparing the results. First, P^{ref} is obtained as for a given instrumented assembly power, which is determined with the option of INCORE-M input that the extrapolation method is not applied only for the instrumented assemblies. Second, P^{ext} is obtained as the extrapolated assembly power of the same fuel assembly without using the measured data of that fuel assembly.

This evaluation was performed with actual operating plant data; however, as noted above, the distribution and relative fraction of measured instrumentation thimbles in the US-APWR is different from the typical Westinghouse-type PWR designs. Since there is no actual measurement data at a plant identical to US-APWR at this time, measurement data from several cycles of a Japanese standard 4-loop PWR is used to evaluate the extrapolation error, simulating the configuration of US-APWR's instrumentation thimble locations (see Figure 5-1).

The "x" symbols in Figure 5-1 indicate the instrument locations that are eliminated intentionally in order to obtain the P^{ext}, as described above. As shown in the figure, the remaining [ ] instrument locations are distributed almost evenly over the core, and the ratio to the total 193 fuel assemblies is [ ] which is equivalent to the US-APWR (14.4%). Although it is not possible to exactly replicate the US-APWR instrumentation locations in a 4-loop plant, the distribution and instrumentation 'coverage' closely simulates the US-APWR.

The next section describes the analyses performed with the modified 4-loop core and the results.

5.3.2 Results

A total[ ]maps for a Japanese 4-loop PWR listed in Table 5-1 were used for the evaluation of the extrapolation error, E^{ext}. The database includes a variety of core types as follows:

[ ]

As an example, extrapolation error results for Cycle 8, BOC, are given in Table 5-2. P^{ref}, P^{ext} and the differences between these values for each location are provided in the table. A summary of the results for each map is given in Table 5-3, and a summary of the results for all maps is provided in Table 5-4 and Figure 5-2. As can be seen, the bias is close enough to zero to be ignored for all the cases.

As shown in Table 5-4, the sample standard deviation of E^{ext} was evaluated to be [ ], where the total number of data used was [ ]. It is important to note that the value of [ ] includes both the extrapolation and measurement reproducibility errors.

5.4 Uncertainties Evaluation of Power Peaking Factors

As summarized in Section 5.2, the measurement uncertainty on $F_{\Delta H}^{N}$ can be obtained by combining the standard deviations of the components (1) to (4), and the uncertainty on F_{Q}^{N} can be obtained by combining components (1) to (6). For convenience, the values for all components are listed below:

Component	s (%)	Degrees of Freedom
(2) Power to Reaction Rate	[	
(3) Extrapolation Uncertainty + (1) Radial Measurement Reproducibility[1]		
(4) Radial Local Peaking		
(5) Elevation Dependent Power to Reaction Rate		
(6) Axial Measurement Reproducibility		]

where, the value of extrapolation uncertainty obtained in the previous section is provided in conjunction with radial measurement reproducibility in the above list[1].

A summary of the evaluations for the uncertainties on $F_{\Delta H}^{N}$ and F_{Q}^{N} is given in Table 5-5. The values of total effective degrees of freedoms are computed to be [ ], respectively. One-sided 95% probability at 95% confidence values of κ corresponding to the effective degrees of freedoms are [ ] respectively, from Reference 6. As results, $F_{\Delta H}^{MU}$, the measurement uncertainty on $F_{\Delta H}^{N}$, is calculated to be [ ] and F_{Q}^{MU}, the measurement uncertainty on F_{Q}^{N}, is calculated to be [ ].

The results show that the power peaking factor uncertainties for the US-APWR are comparable with the evaluation results given in Reference 2, in which $F_{\Delta H}^{MU}$ is [ ] and F_{Q}^{MU} is [ ].

[1] In Reference 2, the extrapolation uncertainty without measurement reproducibility, $E^{ext}_{(w/o\ repro.)}$, is evaluated by "subtracting" the measurement reproducibility from the extrapolation uncertainty that includes measurement reproducibility, $E^{ext}_{(with\ repro.)}$. In this report, they are not divided into two components because they are combined again through the process to obtain uncertainty factors on $F_{\Delta H}^{N}$ and F_{Q}^{N}.

5.5 Uncertainty Factors Determination

As shown in the previous section, the uncertainties on power peaking factors for US-APWR are comparable with those of Westinghouse-type PWRs, although the evaluation results were slightly different to account for the configuration of available measured instrumentation thimbles in the US-APWR.

From the viewpoint of conservatism, the uncertainty factors applied to safety analyses and core surveillance during operation are set to 6% for $F_{\Delta H}^{N}$, and 8% for F_{Q}^{N}, for the US-APWR. The differences between evaluation values and set values are available as margin for the core.

Table 5-1 Cycle and Burnup Used for Extrapolation Uncertainty Evaluation

Table 5-2 Extrapolation Error Evaluation for CY-8, BOC

Table 5-3 Summary of Extrapolation Error Evaluation for Each Map

Table 5-4 Extrapolation Error Evaluation Result

Table 5-5 Summary of Evaluation of Power Peaking Factor Uncertainties

Figure 5-1 Instrument Locations at 4-loop Core that Used for Extrapolation Error Evaluation

[ ]

Figure 5-2 Summary of Extrapolation Error Evaluation

6.0 CONCLUSION

The INCORE-M code is used for the US-APWR to obtain measured power distribution data. INCORE-M is an MHI-modified version of the INCORE code (Reference 1) developed by Westinghouse and widely used in the United States. Both of the codes give the equivalent results, while only INCORE-M code is available for the US-APWR core, which consists of 257 fuel assemblies.

Uncertainty factors must be applied to measured data to account for calculational and measurement uncertainties. Many of the uncertainties applied to the US-APWR using INCORE-M are identical to the values documented in Reference 2. This is because:

- The hardware to measure incore flux is the movable fission chamber detector, which is equivalent to that described in Reference 2,
- The nuclear analysis methodology (References 3, 4, and 5) used for predicted input data is the same as that approved for use with the uncertainties in Reference 2.

However, for the US-APWR, the distribution and relative fraction of measured instrumentation thimbles is different from that of conventional Westinghouse-type PWRs. The power peaking factor uncertainties specific to the US-APWR application are evaluated considering this difference, based on the same methodology discussed in Reference 2. As a result, the measurement uncertainties for $F_{\Delta H}^{N}$ and F_{Q}^{N} are comparable with those of Westinghouse-type PWRs.

Therefore it is conservative and appropriate to use 6% for the uncertainty factor on $F_{\Delta H}^{N}$, and 8% on F_{Q}^{N}, for safety analyses and core surveillance during operation for US-APWR.

7.0 REFERENCES

1. C.E.Meyer and R.L.Stover, Incore Power Distribution Determination in Westinghouse Pressurized Water Reactors, WCAP-8498 (Non-Proprietary), July 1975.
2. Spier, E. M., Evaluation of Nuclear Hot Channel Factor Uncertainties, WCAP-7308-L-P-A (Proprietary), June 1988.
3. Ouisloumen, M. et al., Qualification of the Two-Dimensional Transport Code PARAGON, WCAP-16045-P-A (Proprietary), and WCAP-16045-NP-A (Non-Proprietary), August 2004.
4. Liu, Y.S., et al., ANC - A Westinghouse Advanced Nodal Computer Code, WCAP-10965-P-A (Proprietary), and WCAP-10966-A (Non-Proprietary), September 1986.
5. Nguyen, T. Q., et al., Qualification of the PHOENIX-P/ANC Nuclear Design System for Pressurized Water Reactor Cores, WCAP-11596-P-A (Proprietary), and WCAP-11597-A (Non-Proprietary), June 1988.
6. R. E. Odeh & D. B. Owen, Tables For Normal Tolerance Limits, Sampling Plans, And Screening, 1980.

Appendix-A

Study on the Effect of Instrumentation Thimble Failure for the US-APWR

A.1 INTRODUCTION

This study was performed to evaluate the effect of reducing the available instrumentation thimble locations for the US-APWR, which will be referred to as "thimble deletion" or "thimble failure" in this document. Examples of events that may reduce instrument location availability are damaged or blocked instrumentation thimbles.

The uncertainties on power peaking factors $F_{\Delta H}^{N}$ and F_{Q}^{N} are evaluated in Chapter 5 based on actual operational data from 4-loop PWR plant. As described in Chapter 5, the flux map data were selectively modified to approximate the US-APWR's ICIS design in terms of the instrumented versus uninstrumented assembly ratio, and the distribution of instrumented locations in the core. The analysis to determine the extrapolation error in power distribution measurement was based on the assumption that all instrumented locations in the modified ICIS were available.

An effect to the peaking factors must also be evaluated assuming thimble deletion. However, unlike the extrapolation uncertainty, the influence of thimble deletion is sensitive to the precise geometry of the US-APWR core and instrument locations, and therefore it is not appropriate to use the 4-loop measurement data for this purpose. Because no actual operating data is currently available for the US-APWR design, these uncertainties are derived from comparisons of simulated maps based on 3D core models using the ANC code.

For actual map data, there is always some difference between predicted and measured core power distributions. To simulate differences between predicted data and measured data using only core models, unperturbed core models were used to generate input data for the INCORE-M source deck (predicted powers and reaction rates), and simulated MD data was obtained from perturbed core models (the 'actual core') which provide the simulated measured MD signal data. INCORE-M maps were then generated using this input data.

The effects on $F_{\Delta H}^{N}$ and F_{Q}^{N} are then evaluated based on comparisons between simulated 'reference' map (assuming all thimbles are available) and 'thimble deletion' maps (assuming one or more thimbles are deleted).

Finally, based on an extensive analysis of single and multiple thimble deletion simulations, an approach is developed to minimize the impact of multiple thimble deletions.
Figure A-1 shows the instrumentation thimble deletion reduction process, and the process is explained in detail in the following sections.

A.2 EVALUATION METHOD

A.2.1 Simulated 'Measured' Detector Data Generation

As the basis for providing the predicted and 'measured' MD data, the US-APWR first core and a typical equilibrium reload core were used. The first core and equilibrium reload core represent significant differences in loading patterns; core average burnup and burnup distributions; fuel enrichment; and burnable absorber loading, type, and distributions.

As discussed in the introduction, measured MD signal data based on actual plant operation is always different from the core model predictions (INCORE-M source deck data). Examples of factors which may cause these differences include inherent calculational and measurement uncertainties, actual versus assumed plant operation in the current or previous cycle, etc. To bound these and any other likely causes of differences between predicted and measured data, several perturbations to the unperturbed core model were applied to provide the simulated MD signal data. The perturbation types were chosen to represent both 'normal' conditions, which are actually anticipated to occur, and 'abnormal' conditions that severely perturb the core power distribution. The perturbations were applied at BOC, MOC, and EOC for the first core and the equilibrium core.

Two normal perturbation types were analyzed, assuming control rod misalignment:

Type A : Control Rod Misalignment (insertion)

[ ]

[ ]

Type B : Control Rod Misalignment (withdrawal)

[ ]

Two abnormal conditions were applied to conservatively bound severe perturbations to the core power distribution. One type, Dropped Rod, is an Anticipated Operational Occurrence (AOO) that causes a severe local power distribution perturbation. The other type is an artificial situation which provides an extreme quadrant tilt and thus provides a severe global power distribution perturbation.

Type C : Dropped Rod

[ ]

Type D : Extreme Core Power Tilt

[ ]

In summary, a total of 24 reference cases were generated for the thimble deletion analysis: two cycles (first core and equilibrium core), with four perturbations (Types A-D) on each core at BOC, MOC and EOC. The 24 reference cases are summarized in Table A-1.

An example of perturbation case is shown in Figure A-2, which is for Case No.8 of Table A-1: Cycle 1, MOC, with a Type D perturbation (Extreme Core Power Tilt). The figure shows a comparison of assembly power distribution before and after the perturbation, as well as a comparison of power peaking factors ($F_{\Delta H}^{N}$ and F_{Q}^{N}). The maximum difference in assembly power in this case is [ ] and the $F_{\Delta H}^{N}$ and F_{Q}^{N} increases due to this hypothetical perturbation are [ ] and [ ] respectively. As described above, the MD data created based on this kind of perturbed core model are input to the thimble deletion simulation.

A.2.2 Thimble Deletion Simulation

Using the simulation calculations described in the previous section, simulated MD signals are provided for all 37 instrumentation thimble locations for each of 24 cases listed in Table A-1, for use in INCORE-M. The unperturbed core model provides the source deck information for the predicted data: [ ] etc. The perturbed core model provides the 'measured' thimble fluxes. The INCORE-M map with no instrument deletions is the 'reference map'. Thimble failures can be easily simulated by deleting the MD signals for one or more instrument thimbles from the reference map INCORE-M input. In this way, four scenarios of thimble deletion were simulated for each of the 24 reference cases listed in Table A-1: one, two, three and five thimble deletions were assumed. For the single deletion cases, [ ] For multiple thimble deletion scenarios, [ ]

For the five-deletion scenario, [ ] The results of the thimble deletion cases (change in maximum $F_{\Delta H}^{N}$ and F_{Q}^{N}) were compared to the reference map results to evaluate the influence of thimble reduction.

Based on an analysis of the results, it was found that some combinations of thimble deletions produced unacceptably large decreases in measured peaking factors, which is non-conservative because the measured value is underestimated at thimble failure condition. As expected, these cases were situations in which thimble failures were 'clustered'. Statistically, these situations are very unlikely to occur in actual operation. To avoid unnecessarily large effect to measured peaking factors, a limitation on the allowable proximity of thimble failures was developed. Based on the US-APWR instrumentation configuration, no thimble failure is permitted within a circular area with a radius of $\sqrt{10}$ assembly pitches with respect to another thimble failure, as shown in Figure A-3. This limitation provides a general rule for thimble failure allowances for core monitoring, and is discussed further in Section A.4.

Using this limitation, the results of the instrumentation thimble deletion cases were 'filtered' to eliminate any situations that did not meet the proximity criteria. Table A-1 shows the number of cases analyzed for each condition which meet the proximity criteria. These cases were used for the evaluation.

A.3 RESULTS

As shown in Table A-1, an extensive number of simulations have been performed for each thimble deletion scenario. Figures A-4 through A-7 show examples of simulation results for thimble deletion scenarios for case No.8 in Table A-1 again (First core, MOC, Type D perturbation) for one, two, three, and five thimble deletions, respectively. The figures include comparisons of reference case and deletion case assembly power, as well as the peaking factor comparisons.

The effects of single and multiple thimbles deletion on $F_{\Delta H}^{N}$ and F_{Q}^{N} measurements are summarized in Figures A-8 and A-9 for all the cases simulated. These figures show that [ ] and there is the limitation that no thimble failure is permitted within a circular area with a radius of $\sqrt{10}$ assembly pitches with respect to another thimble failure as described in Section A.2.2. This limitation prevents the use of measurement results that lack sufficient information for peak power locations. As shown in Figures A-8 and A-9, the maximum impact on measured peaking factors due to thimble failure is [ ] for $F_{\Delta H}^{N}$, and [ ] for F_{Q}^{N}, up to five failed thimbles.

A.4 CONCLUSION

An extensive number of simulations of power distribution measurements have been performed to evaluate the impact of single or multiple thimble deletions on $F_{\Delta H}^{N}$ and F_{Q}^{N} measurement using simulated thimble signals provided by core models. The simulations are based on reference cases that include perturbations to the core to represent differences between predicted and measured core power distributions prior to thimble deletion.

The result of the simulations, which include both normal conditions and abnormal conditions, shows that the maximum impacts on $F_{\Delta H}^{N}$, and F_{Q}^{N} measurement are [ ] respectively, on the assumptions listed below:

1) The number of unavailable (failed) thimbles is no greater than five,
2) No thimble failure occurs within a circular area with a radius of $\sqrt{10}$ assembly pitches with respect to another thimble failure.

It is described in Chapter 5 of this report that the uncertainty factors, $F_{\Delta H}^{MU}$ and F_{Q}^{MU}, have been evaluated as [ ] respectively, for the US-APWR ICIS design without considering the effect of thimble failure, and the factors applied for the safety analyses are conservatively set to 6% and 8%, respectively. The margins between evaluated values and set values are large enough to allow the impacts of thimble failure on $F_{\Delta H}^{N}$ and F_{Q}^{N} measurement, since the uncertainty factors $F_{\Delta H}^{MU}$ and F_{Q}^{MU} are statistically independent to the impacts of thimble failure, direct addition of these effects is a conservative treatment.

Therefore, it is concluded that the impacts of thimble failure on $F_{\Delta H}^{N}$ and F_{Q}^{N} measurement can be accommodated within the margin of the uncertainty factors, if the two conditions described above are met.

Table A-1 Summary of Simulation Cases

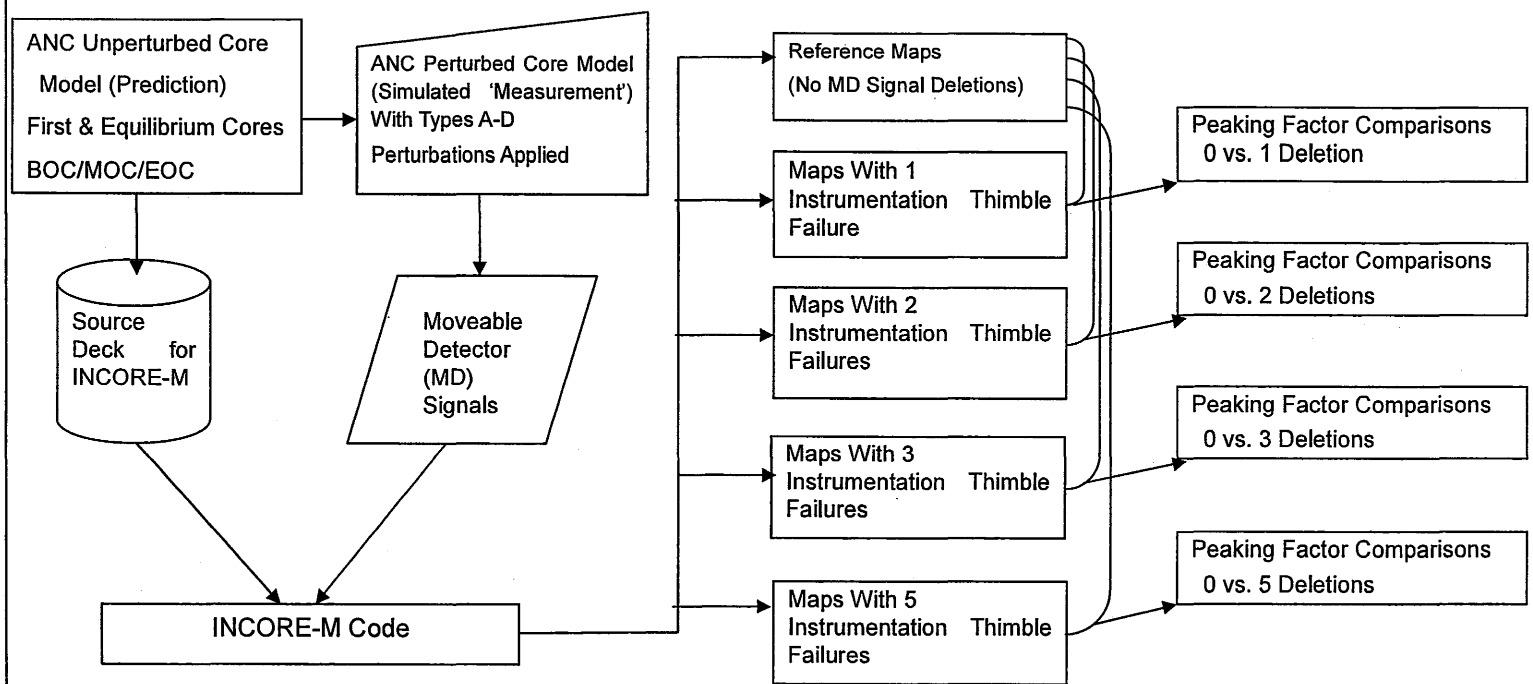

Figure A-1 Instrumentation Thimble Reduction Evaluation Process

Figure A-2 A Comparison of Assembly Power Distribution between Unperturbed Core model and Perturbed Core model (First Core, MOC, Type-D Perturbation)

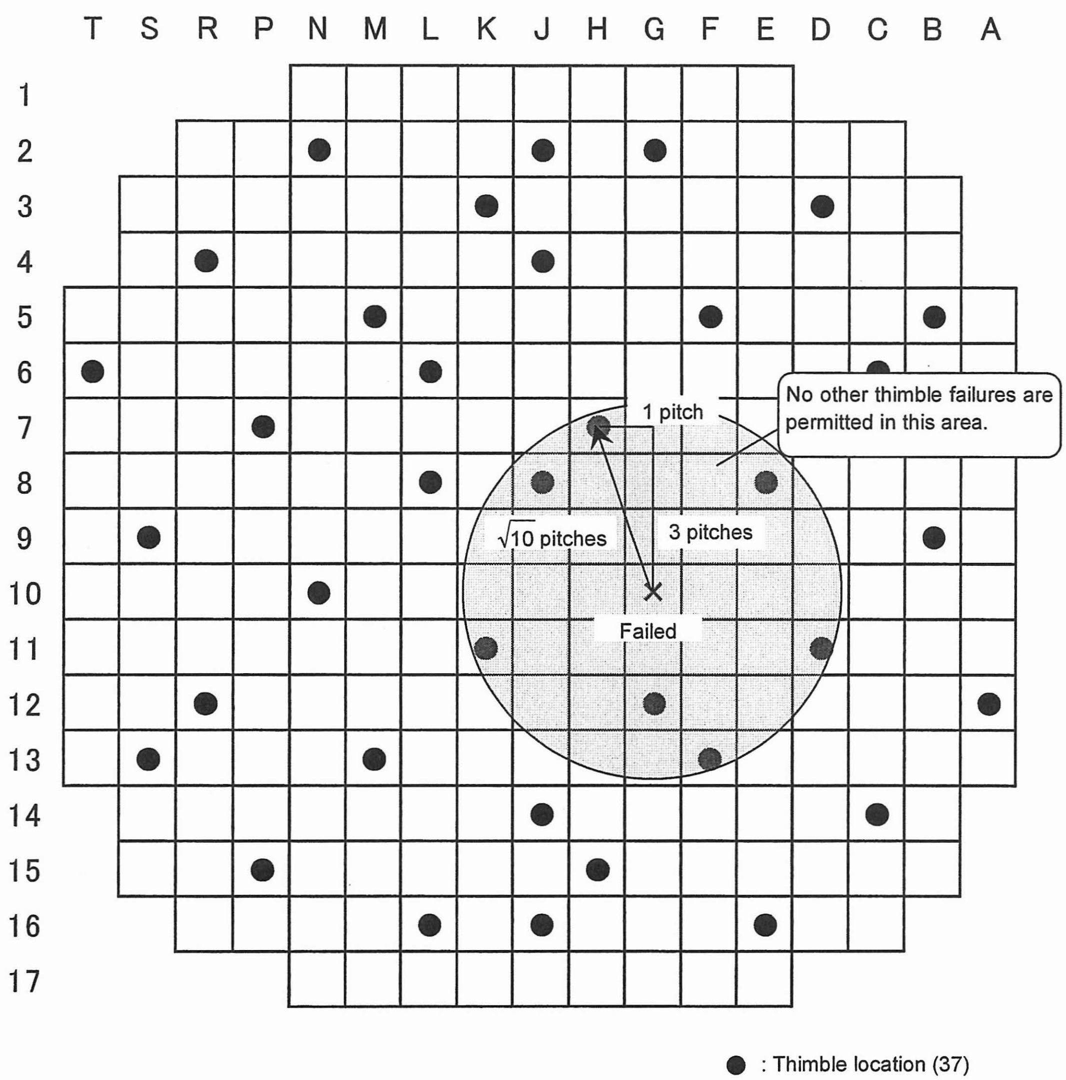

Figure A-3 Example of Proximity Limitation for Thimble Failures

Figure A-4 A Comparison of Measured Assembly Power Distribution between Reference Case and Thimble Deletion Case (First Core, MOC, Type-D Perturbation, 1 Thimble Failure)

Figure A-5 A Comparison of Measured Assembly Power Distribution between Reference Case and Thimble Deletion Case (First core, MOC, Type-D Perturbation, 2 Thimbles Failure)

Figure A-6 A Comparison of Measured Assembly Power Distribution between Reference Case and Thimble Deletion Case (First Core, MOC, Type-D Perturbation, 3 Thimbles Failure)

Figure A-7 A Comparison of Measured Assembly Power Distribution between Reference Case and Thimble Deletion Case (First Core, MOC, Type-D Perturbation, 5 Thimbles Failure)

Figure A-8 Summary of the Analyses Results: Maximum %Decrease in Measured $F_{\Delta H}^{N}$ between Reference Case and Thimble Deletion Cases

Figure A-9 Summary of the Analyses Results: Maximum %Decrease in Measured F_Q^N between Reference Case and Thimble Deletion Cases